

Performance of Multicast Packet Aggregation in All Optical Slotted Networks

Hind Castel-Taleb, Mohamed Chaitou, and Gerard Hébuterne

INSTITUT TELECOM, TELECOM SudParis
9, rue Charles Fourier 91011 Evry Cedex, France
`hind.castel@it-sudparis.eu`

Abstract. The study focuses on packet aggregation mechanisms on the edge router of an optical network. The device works as an interface between the electronic and optical domains : it takes IP packets coming from client layers and converts them into optical packets to be sent into the optical network. An efficient aggregation mechanism supporting QoS (Quality of Service) requirements of IP flows is presented. A timer is implemented to limit the aggregation delay. Analytical models based on Markov chains are presented in order to study the packetisation efficiency (filling ratio) and the mean time of packetisation for each class. Numerical results show the effect of IP packet lengths distribution on aggregation delay and efficiency. Also, we show the importance of the timer in bounding the delay of transmitted packets without much altering the aggregation efficiency.

Keywords: Optical networking, Packet aggregation, Bandwidth efficiency, Quality of service (QoS), Traffic engineering.

1 Introduction

In recent years, considerable research has been devoted to design IP full optical backbone networks, based on Wavelength Division Multiplexing (WDM) technology [10], in order to relieve the capacity bottleneck of classical electronic-switched networks. In a long-term scenario, the optical packet switching (OPS), based on fixed-length packets and synchronous node operation, can provide a simple transport platform based on a direct IP over WDM structure which can offer high bandwidth efficiency, flexibility, and fine granularity [26]. In [24], both client/server and Peer to Peer traffics are studied in order to study the impact of traffic profiles on the performance of the system. Two major challenges face the application of packet switching in an optical domain. First, the adaptation of IP traffic, which mainly consists of asynchronous and variable length packets, with the considered synchronous OPS network. Second, the handling of QoS (Quality of Service) requirements in the context of a multi-service packet network. To cope with the first problem, IP packet aggregation at the interface of the optical network ([8,15,6]) presents an efficient solution among few other proposals in literature ([22,2]).

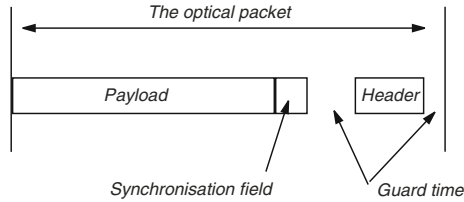


Fig. 1. Optical packet format

This is because in the current OPS technology, a typical guard time of 50 ns must be inserted between optical packets [12]. Also, a synchronisation field is to be provided, so that the optical packet is built as in Fig.1. In any packet switching network, information is carried and processed in blocks, incorporating the useful *payload* and the *header* needed to process and forward the packet through the network. Different packet formats are defined, which impact the mean delays in the optical MAN [7]. As the header has no usefulness from the end-to-end viewpoint, it corresponds to a portion of the total bandwidth which may be seen as wasted and thus its relative importance has to be minimized, which calls for rather long packets.

A possible issue is the aggregation of several IP packets into a single macro-packet with fixed size, which represents an aggregate optical packet. Furthermore, it is necessary to perform the aggregation process regardless of the destinations of IP packets. This is due to the permanent increase in the number of IP networks, and consequently, in the number of destinations, which leads to a poor filling ratio of the optical packet if the aggregation process is performed by destination (i.e., IP packets with same destinations are aggregated together). The QoS problem is treated by adopting a class-based scheme in the edge nodes, which simplifies the core of the optical network by pushing the complexity towards the edge nodes.

According to the above discussion, this paper proposes aggregation mechanisms in order to aggregate variable-length IP packets into the payload of an optical packet. In the first mechanism proposed, the aggregation cycle ends if the aggregated packet cannot accommodate more IP packets. We present the analytical based on Markov chains in order to evaluate performance measures as packetisation delay and efficiency. Analytical results show clearly the influence of IP packet lengths on performance measures. Secondly, we introduce in the aggregation mechanism the QoS requirements of IP flows, and timer. In this second mechanism, variable-length and multi-CoS (Class of Service) IP packets are aggregated regardless of their final destinations.

The idea consists of the separation of IP traffic into $\{J \geq 2\}$ prioritized queues according to the desired CoS. At each fixed interval of time (τ), an aggregation cycle begins and an aggregate packet is constructed from several IP packets belonging to the different queues. In addition, we apply an aggregation priority mechanism by collecting IP packets, at the beginning of each aggregation cycle,

from higher priority queues before those of lower priority. However, in order to relieve the drawbacks of such strict priority discipline, an hybrid version of the probabilistic priority algorithm presented in [16,17] may be used. Since the size of an IP packet at the head of a queue i , $\{1 \leq i \leq J\}$ may be greater than the gap remaining into the aggregate packet, the IP packet can be segmented in this case.

The second aggregation technique exhibits two particular characteristics. First, an aggregate packet is generated at regular time intervals, which may vary dynamically in order to sustain a prefixed amount of the filling ratio [19]. Second, a multicast optical packet is constructed. We present possible applications of such aggregation method in MANs and WANs respectively. As candidate applications in MANs, we mention the family of slotted ring networks deploying destination stripping such as the network studied in [21]. In addition, a broadcast network, which is a slotted version of the multi-channel packet-switched network called DBORN (Dual Bus Optical Ring Network) [20], represents an important application. This is because DBORN matches very well the multicast nature of the generated optical packets without the addition of any complexity in the node architecture. Furthermore, DBORN, coupled with the aggregation technique, can be adapted to use an access scheme based on TDMA, but avoids the lack of efficiency exhibited by the latter in the case of unbalanced traffic.

The present paper is organized as follows. The first aggregation mechanism is presented in section 2. Using a mathematical analysis, we give the packetisation efficiency and delay. We present analytical results in order to see the impact of packet length distribution on the packetisation mechanism. In section 3, we introduce the second aggregation mechanism with different QoS levels. Moreover, a timer is implemented in order to limit the aggregation delay. We present the analytical model in order to compute the aggregation delay for each class. Some numerical examples are presented and commented. Sections 4 and 5 explain how to apply the aggregation technique to MANs and WANs, respectively. Finally, Section 6 concludes the paper.

2 The First Packet Aggregation Mechanism

The study considers the aggregation of blocks of data in a single packet. The typical application is the building of optical packets in the edge router of optical backbone: IP packets, of variable length, are put together in fixed-size packets before being sent in the network. Most often an Ethernet link is used so that IP packets are segmented according to the maximum size of Ethernet frames. For convenience, the entering packets from the client layer are named "blocks", while the term of "packet" is reserved to the constant-size optical packet. The operating mode is as follows:

- Individual blocks, with variable length, arrive in the aggregation unit. The block is tentatively inserted in the packet under building.
- If there is enough room for the block, the packet remains in the unit until next block. If the block cannot be inserted because of its size, then the

current packet is considered as being completed and is sent in the network. The arriving block is denoted as a *trigger block*, as it provokes the packet sending. The part of the packet which is still not filled is wasted. At the same time a new packet is created, and the trigger block is inserted in it.

- When a new packet is created, a time-out is initialized. If the time-out fires before the packet is completed, the packet is immediately sent, whichever its current filling.

There are two problems related with this process, namely the choice of the packet size and the choice of the time-out value. The point is that long packets yield an optimal use of the available bandwidth, at the price of an increasing end-to-end delay, while too short packets increase the burden of headers and wasted bandwidth resource.

2.1 Mathematical Analysis

Let the individual blocks have their lengths distributed according to a common probability distribution function F , with density f . The successive block sizes are independent and identically distributed (i.i.d.). Let m be the average block length. The constant size of the optical packet is denoted as K . The units for measuring K or the block lengths may be either bits, or bytes, or larger units. For the analysis of delay performance, one has to specify the arrival process of the client blocks. When needed, one assumes they arrive according to a Poisson process, with rate λ .

In a time interval T , λT blocks arrive, which represent a total amount of $\lambda T m$ bits. They will be sent in $N(T)$ packets, carrying both the useful data, the header information and the padding bits. Let E denote the average pad length. The average number of blocks per packet, p , gives the average useful payload pm (using Wald’s relation proves this result), which is related with the average waste, by the relation : $E + pm = K$.

The packetisation efficiency ϵ is defined as the ratio of the average filled payload to the total payload length :

$$\epsilon = \frac{pm}{K} \tag{1}$$

$N(T)$ is given by the simple relation :

$$N(T) = \frac{\lambda T}{p} \tag{2}$$

The average packetization delay θ is related with p : the packet begins with block 1 and is sent when block $p + 1$ arrives, representing thus p interarrival periods. So the average delay θ is equal to:

$$\theta = \frac{p}{\lambda} \tag{3}$$

If D represents the bandwidth (in bit/second), then $D = \lambda m$, and we obtain that:

$$\theta = \frac{pm}{D} \tag{4}$$

A model for packet length. The study considers the process (X_n) of the cumulated packet size after the arrival of the n -th block (whether the optical packet is sent or not). Let $H_n(x)$ denote the probability distribution function of the (X_n) . The process (X_n) is a discrete-time Markov process, which obeys the following recurrence relation (f_n stands for the size of the n -th arriving block):

$$X_n = \begin{cases} X_{n-1} + f_n & \text{if } X_{n-1} + f_n \leq K \\ f_n & \text{otherwise} \end{cases} \tag{5}$$

The above recurrence yields the following relation between pdf's :

$$P\{X_n \leq x\} = \int_{y=0}^x f_n(y)P\{X_{n-1} > K - y\} dy + \int_{y=0}^x f_n(y)P\{X_{n-1} \leq x - y\} dy \tag{6}$$

Now, we assume that a stationary limit exists. This gives the fundamental relation:

$$H(x) = \int_{y=0}^x f(y)[1 + H(x - y) - H(K - y)] dy \tag{7}$$

From the solution of the precedent equation , the major performance figures are derived. Especially, the distribution of the packet size is of prime importance. Let $Q(x)$ be the probability that a packet is sent with size lower or equal to x . First, the probability Π that a packet is sent at epoch n is equal to the probability that the n -th arriving block is a “trigger block”. So:

$$\Pi = \int_{y=0}^K f(y)[1 - H(K - y)] dy \tag{8}$$

Now, Q is derived from H : this is the probability that the X_n is lower than x , given that a packet is actually sent:

$$Q(x) = P(X_{n-1} \leq x \text{ and } f_n \text{ trigger block} | \text{a packet is sent at } n - 1) \tag{9}$$

So:

$$Q(x) = \frac{1}{\Pi} \int_{u=0}^x \int_{y=K-u}^K dy H(u) f(y) dy = \frac{1}{\Pi} \int_{y=K-x}^K f(y) [1 - H(K - y)] dy \tag{10}$$

The case where block sizes have a discrete distribution. When the f_n take only discrete values, a simpler set of equations may be used. First, one can assume that the distribution of the arriving block is an integer multiple of a basic block (a byte, or more – e.g. 64 bytes). In this case, all the problem is reformulated using the basic block as unit. The packet size K is then expressed as an integer number of basic blocs. The recurrence relation (5) is still valid, but it allows a more tractable one-dimension Markov chain formulation. Especially, $H(x)$ is given by:

$$H(x) = \sum_{y=0}^x P\{f = y\}[1 + H(x - y) - H(K - y)] \tag{11}$$

As (X_n) can take only discrete values, the following relation holds: $P \{X_n = x\} = H(x) - H(x - 1)$, which is equal to:

$$\sum_{y=0}^x P \{f_n = y\} P \{X_n = x - y\} + P \{f_n = x\} P \{X_n > K - x\} \quad (12)$$

This relation corresponds to the local balance equation on state $\{X_n = x\}$. In other words, in the case of discrete values of ingoing blocks, the relations given for $H(x)$ generate the resolution of the discrete Markov chain which governs the evolution of (X_n) . Let us explain now how to compute performance measures, such as the mean size of the payload of optical packets, and the average packetisation delay. We must give $Q(x)$ in the case of discrete size of packets : it will represent the probability that a packet of size $x \in N$ will be sent. The relations given in the continuous case still hold. First let us write Π , the packetization probability, which becomes in the discrete case:

$$\Pi = \sum_{y=0}^K P \{f = y\} [1 - H(K - y)] \quad (13)$$

So $Q(x)$ is given by the following relation :

$$Q(x) = \frac{\sum_{y>K-x} P \{f = y\} P \{X = x\}}{\Pi} \quad (14)$$

Let N be the mean size of the effective payload in optical packets :

$$N = \sum_{x=0}^K x Q(x) \quad (15)$$

The packetisation efficiency ϵ is :

$$\epsilon = \frac{N}{K} \quad (16)$$

The average packetization delay θ is :

$$\theta = \frac{N}{m\lambda} \quad (17)$$

which is equivalent to :

$$\theta = \frac{N}{D} \quad (18)$$

2.2 Numerical Results

In this section, we give some numerical results in order to see the performance of packet aggregation. We suppose that the block sizes have a discret distribution, and we compute the packetisation efficiency and the mean time of packetisation, using equations given in section 2.1.

Table 1. Block length distributions

C_i	64 bytes	576 bytes	1600 bytes
C_1	0.25	0.75	0
C_2	0.25	0.5	0.25
C_3	0.25	0.25	0.5
C_4	0.25	0	0.75

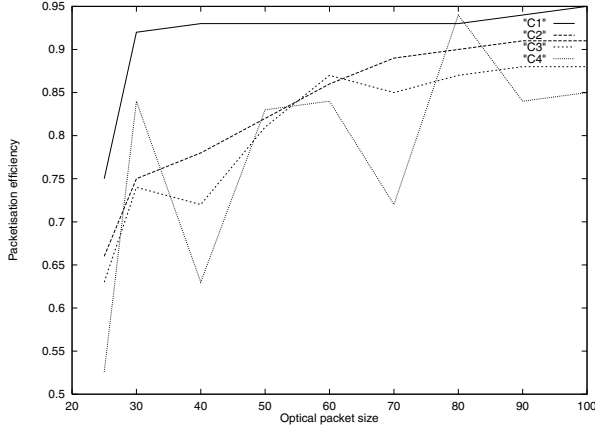


Fig. 2. Packetisation efficiency versus optical packet size

In Fig.2, we have plotted several curves representing the packetisation efficiency versus the optical packet size. For all the experiments, we have supposed that the arrival rate λ of clients IP blocks is $10/\mu s$, and the unit for measuring the block lengths and optical packet size K is 64 bytes. Performance measures are computed for optical packet sizes varying from 1600 bytes to 6400 bytes (25 packet units to 100 packet units in figures). We have supposed different block length probability distributions for input IP packet flows.

The curve " C_i " for $i \in [1 \dots 4]$ corresponds to the C_i configuration for the block length distribution. We have chosen block lengths equal to : 64 bytes, 576 bytes, and 1600 bytes. In table 1, we give block length distributions of IP packet flows for each C_i .

We notice that when the ratio of blocks with a high length increases, then the packet efficiency decreases. For the curve " C_4 ", we can remark an oscillation phenomenon : as we have often arrivals of large length block then we have two cases : the packet is either well filled, or not (he has an important free places but not enough to be filled with the block). Except for this case, we can see that the block length distribution has not an important impact on the packetisation efficiency. As it seems that current IP flows exhibit a rather high proportion of short IP packets (acknowledgements typically), configurations " C_1 " and " C_2 " are the most likely to be observed. However, the partial filling effect is to be mixed with the bandwidth waste related to guard bands and headers. Assume

Table 2. Global performance figures

Payload length	Packet duration	Global efficiency
1600 bytes	1.48 μ s	0.57
3200 bytes	2.76 μ s	0.77
6400 bytes	5.32 μ s	0.87

for instance that they result in a 200 ns (100 ns for guard times and 100 ns for the header), and that the link speed is 10 Gbits/s. In table.2 we give the following global performance figures in the case of the (probably most typical) configuration "C₂".

In Fig.3, we show the mean packetisation delay (in μ s) versus the optical size. As can be expected, the longer the packet, the longer the aggregation delay. Also, as the aggregation efficiency increases, so does the delay-since more data is needed to fill the packet. Therefore, efficiency is obtained at the price of additional delay. We can see in this figure, that for an optical packet size of 1600 bytes, the packetisation delay varies from 0.26 μ s (curve C1) to 0.069 μ s (curve C4). And for 6400 bytes it varies from 1.358 μ s (curve C1) to 0.45 μ s (curve C4). So we deduce that the delay is quite negligible for $\lambda=10$ blocks/ μ s, but it increases if λ decreases (for $\lambda=10$ blocks/s, the delay will have the same values but given in secondes). Suppose now that the flow to carried through the aggregation process is 1Gbits/s (so $D=1$ Gbits/s), we obtain the following values of the mean packetisation delay given in table 3.

We can see that for $D=1$ Gbit/s, the delay is quite negligible, but as for λ , if D decreases, the delay increases.

We have proposed in this section a first mechanism for packet aggregations, and we have evaluate the performance using mathematical models. This system is not very complex, We have seen the impact of packet length distributions on

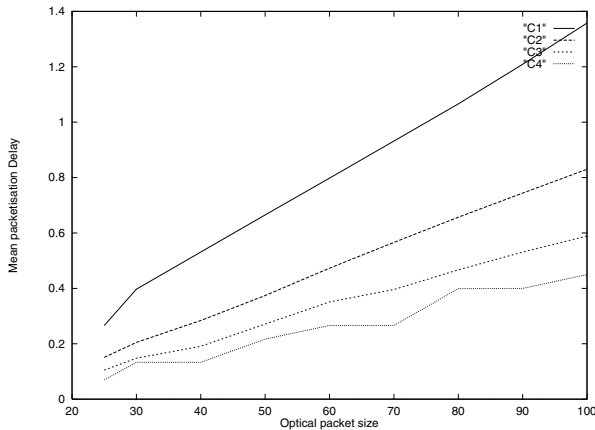


Fig. 3. Average packetisation delay in μ s versus optical packet size

Table 3. Packetisation delay in μs for 1 Gbit/s flow

Payload length	C1	C2	C3	C4
1600 bytes	1.19	1.06	1.01	0.84
3200 bytes	2.98	2.64	2.60	2.64
6400 bytes	6.09	5.84	5.67	5.48

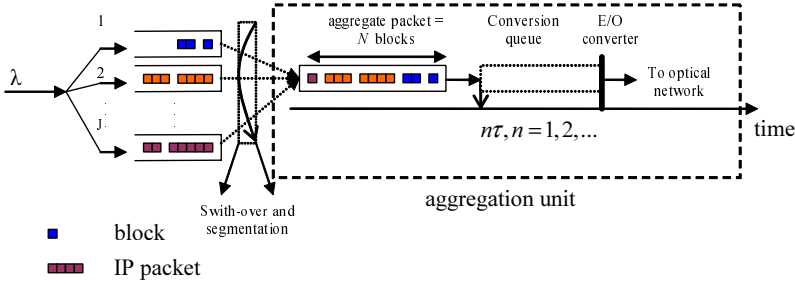


Fig. 4. The aggregation mechanism at the optical interface

packetisation delay and efficiency. Furthermore, we need to complexify the aggregation mechanism by introducing a timer parameter, and taking into account QoS of different packet flows.

3 The Second Packet Aggregation Mechanism

Let there be J classes of packets (throughout the paper the term "packet" stands for "IP packet"), where packets with a smaller class number have a higher priority than packets with a larger class number. Each class of packets has its own queue and the buffer of the queue is infinite. Packets in the same queue are served in FCFS fashion.

3.1 Mathematical Model

Each packet is modeled by a batch of blocks having a fixed size of b bytes. Let X be the batch size random variable with probability generating function (PGF) $X(z)$, and probability mass function (pmf) $\{x_n = P(X = n), n \geq 1\}$. The size of the aggregate packet is fixed to N blocks ($N > \max(X)$), and a timer with a time-out value τ is implemented as shown in Fig. 4. At each timer expiration (i.e at instants $\{n\tau, n = 0, 1, 2, \dots\}$) the aggregation unit takes $\min(N, \text{the whole queue 1 length})$ blocks to attempt filling the aggregate packet. If a gap still remains, the aggregation unit attempts to fill it from queue 2, then from queue 3, ..., until the aggregate packet becomes full or until queue J is reached. If the whole of the IP packet cannot be inserted (e.g., the packet at the head of queue J in Fig. 4), only a part of it, needed to fill the aggregate packet, is

transferred to the aggregation unit (a segmentation interface performs packets segmentation just before the aggregation unit). The aggregate packet is then sent to a queue (called conversion queue) preceding the stage of the electronic to optical conversion (E/O), and a new aggregation cycle is performed by polling queue 1 again. Note that in the discipline described above, it may take several times for the aggregation unit to switch from one queue to the other to actually perform packets aggregation in each aggregation cycle. Throughout the rest of this paper, we assume that the switch-over time can be much small as compared to the sojourn time and will not be taken into account in the analysis. It is worthwhile mentioning that the discrimination between successive IP packets, contained in an aggregate packet, is performed by using a delineation protocol such as the protocol proposed in [11].

In the analytical study, we first begin by considering only two classes of packets ($J = 2$). However, the analysis can be extended easily to a multi-class system, as it will be shown later. The following assumptions and notations are used throughout this paper. We assume that packets arrive at the corresponding queues according to independent Poisson processes with rates λ_1 and λ_2 , i.e. the total arrival rate is $\lambda_0 = \lambda_1 + \lambda_2$. We define $\{A_t^c, c = 0, 1, 2\}$ as the number of blocks arriving at queue c , (for $c = 0$ the queue corresponds to the combination of queues 1 and 2), during an interval of time t , and we design by $\{A_t^c(z) = e^{\lambda_c t (X(z)-1)}\}$ its PGF and $\{a_t^c(n), n \geq 0\}$ its pmf.

3.2 Blocks Number Pre-departure Probabilities and Filling Ratio

We define $\{Y^c(t), c = 0, 1, 2\}$ by the number of blocks in queue c at time t , and we suppose that $Y_n^c = Y^c(t_n^-)$. We choose a set of embedded Markov points as those points in time which are just before timer expirations. Let $t_0, t_1, \dots, t_n, \dots$, be the epochs of timer expirations. Since the whole system and queue 1 behave in a similar way, the steady state distribution for $\{Y_n^c, n = 0, 1, 2, \dots\}$ is obtained by the same manner for $\{c = 0, 1\}$:

$$y_k^c = \lim_{n \rightarrow \infty} P(Y_n^c = k), \quad k \geq 0 \tag{19}$$

The following state equation holds:

$$Y_{n+1}^c = |Y_n^c - N|^+ + A_\tau^c \tag{20}$$

where $|c|^+$ denotes $\max(0, c)$. The equilibrium queue length distribution (in blocks number) at an arbitrary time epoch is then described by the probability generating function $Y^c(z)$, which can be derived in (21) by a straightforward and well-known fashion [9]. It is given by :

$$Y^c(z) = \frac{A_\tau^c(z)(z-1)(N-E[A_\tau^c])}{z^N - A_\tau^c(z)} \prod_{k=1}^{N-1} \frac{z-z_k}{1-z_k} \tag{21}$$

where, z_1, z_2, \dots, z_{N-1} are the $N - 1$ zeros of $z^N - A_\tau^c(z)$ inside the unit circle of the complex plane, and $E[\dots]$ is the expectation value of the expression between square brackets. Using the inverse fast fourier transform (ifft) of MATLAB, y_n^c can be derived from (21) in few seconds. Equation (21) allows us to obtain the pmf of the aggregate packet filling value (i.e the number of blocks in the aggregate packet). Let F be the filling value random variable, and define the filling ratio random variable by $F_r = F/N$ (which is equivalent to the bandwidth efficiency). If we denote by $\{f_n = P(F = n), 0 \leq n \leq N\}$ the pmf of F , we obtain:

$$f_n = \begin{cases} y_n^0 & \text{if } 0 \leq n < N - 1 \\ 1 - \sum_{i=0}^{N-1} y_i^0 & \text{if } n = N \end{cases} \tag{22}$$

To obtain the steady state distribution for $\{Y_n^2, n = 0, 1, 2, \dots\}$, the state equation can be written as:

$$Y_{n+1}^2 = |Y_n^2 - G|^+ + A_\tau^2 \tag{23}$$

where G represents the gap random variable. It is given by $G = N - F$, and hence, its pmf defined by $\{g_n, n = 0, 1, 2, \dots, N\}$ can be obtained easily from (22). The PGF of Y^2 is then given by (see [9]):

$$Y^2(z) = \frac{A_\tau^2(z)(z - 1)(N - E[U])}{z^N - U(z)} \prod_{k=1}^{N-1} \frac{z - z_k}{1 - z_k} \tag{24}$$

where U is the random variable defined by: $U = N + A_\tau^2 - G$, and z_1, z_2, \dots, z_{N-1} are the $N - 1$ zeros of $z^N - U(z)$ inside the unit circle.

Blocks number random instant probabilities. Let $\{K^c, c = 1, 2\}$ denote the number of blocks, at a random instant t , in queues 1 and 2 respectively , and let $\{q_k^c = P(K^c = k), k \geq 0\}$ be its pmf.

Lemma 1. K^c is related to Y^c by:

$$K^c(z) = Y^c(z) \frac{1 - e^{-\lambda\tau(X(z)-1)}}{\lambda\tau(X(z) - 1)} \tag{25}$$

Proof: The proof is given for $c = 2$, the case of $c = 1$ is a particular case obtained by replacing the random variable G (the gap) with the constant parameter N (the length of the aggregate packet). Let T_e be the elapsed time since the last timer expiration. By conditioning on T_e , the following state equation can be obtained:

$$K^2 | (T_e = t) = |Y^2 - G|^+ + A_\tau^2 \tag{26}$$

Then (superscript 2 is omitted for simplicity), if we denote by $K^* = K(z | T_e = t)$ is given by:

$$\begin{aligned} K^* &= \sum_{k=0}^\infty P[|Y - G|^+ + A_t = k] z^k \\ &= \sum_{k=0}^\infty \sum_{i=0}^N g_i P[|Y - i|^+ + A_t = k] z^k \\ &= \sum_{k=0}^\infty \sum_{i=0}^N g_i \left\{ \sum_{j=0}^i y_j P[A_t = k] + \sum_{j=i+1}^\infty y_j P[A_t = k - j + i] \right\} z^k \\ &= A_t(z) \left\{ \sum_{i=0}^N g_i \left(\sum_{j=0}^i y_j + z^{-i} \left(Y(z) - \sum_{j=0}^i y_j z^j \right) \right) \right\} \end{aligned} \tag{27}$$

With (see [9])

$$\begin{aligned}
 \left(\sum_{i=0}^N g_i \sum_{j=0}^i y_j - \sum_{i=0}^N g_i z^{-i} \sum_{j=0}^i y_j z^j \right) &= \frac{Y(z)(1-A_\tau(z) \sum_{i=0}^N g_i z^{-i})}{A_\tau(z)} \Rightarrow \\
 K(z \mid T_e = t) &= \frac{A_t(z)}{A_\tau(z)} Y(z)
 \end{aligned}
 \tag{28}$$

To obtain $K(z)$, it is sufficient to remove the condition on T_e , thus,

$$K(z) = \int_{t=0}^\tau \frac{A_t(z)}{A_\tau(z)} Y(z) \left(\frac{dt}{\tau} \right)
 \tag{29}$$

and the proof is completed.

3.3 Mean Delay Analysis

In this section we present a method to obtain the mean aggregation delay of an IP packet belonging to class 1 or to class 2. The aggregation delay random variable of a class c packet, $\{c = 1, 2\}$, is represented by $\{D^c, c = 1, 2\}$, and it is defined as the time period elapsed between the arrival instant of the packet to its corresponding queue, and the instant when the last block of the packet leaves the queue. The delay can be decomposed in two parts: the waiting time of the packet first block until it becomes at the head of the queue, and the delay due to the packet segmentation when the packet cannot be inserted directly into the remaining gap of the aggregate packet. The decomposition is written, in term of mean delays, as:

$$E[D^c] = E[D_b^c] + D_s^c
 \tag{30}$$

where D_b^c denotes the packet first block waiting time in the queue and D_s^c stands for the packet segmentation delay. By using the Little theorem we get:

$$E[D_b^c] = \frac{E[K^c]}{\lambda_c \times E[X]}
 \tag{31}$$

where $E[K^c]$ can be obtained by putting $z = 1$ in the first derivative of $K^c(z)$, and its given by:

$$\begin{aligned}
 E[K^c] &= E[Y^c] - \frac{\lambda_c \tau E[X]}{2} \\
 &= \left\{ E[A_\tau^c] + \left[\frac{VAR[C(U, A_\tau^1)]}{2(N-E[C(U, A_\tau^1)])} - \frac{E[C(U, A_\tau^1)]}{2} + \frac{1}{2} \sum_{k=1}^{N-1} \frac{1+z_k^c}{1-z_k^c} \right] \right\} - \frac{\lambda_c \tau E[X]}{2}
 \end{aligned}
 \tag{32}$$

with,

$$C(x, y) = \begin{cases} x & \text{if } c = 1 \\ y & \text{if } c = 2 \end{cases}
 \tag{33}$$

$VAR[X]$ is the variance of X , $\{z_k^1, 1 \leq k \leq N - 1\}$ and $\{z_k^2, 1 \leq k \leq N - 1\}$ are the roots inside the unit circle of the two respective following equations: $\{z^N - A_\tau^1(z)\}$ and $\{z^N - U(z)\}$, with $U(z)$ defined in section 3.2. Note that the roots are found using a numerical method with a precision of 10^{-10} .

Computation of D_s^1 . We consider the case where $N > \max(X)$, where X denotes the batch size random variable (i.e the size of an IP packet in term of blocks), which implies that a class 1 packet cannot be segmented more than once. If we denote by $p_s^{1,n}$ the probability that a packet is segmented n times, then the segmentation delay of a class 1 packet will be given by:

$$D_s^1 = \sum_{n=1}^{\infty} p_s^{1,n} \times (n\tau) = p_s^{1,1} \times \tau \tag{34}$$

The following is a method to obtain $p_s^{1,1}$: let N_s be the random variable representing the number of blocks that enters the aggregation unit before the first block of a random packet, given that the latter (the first block of the packet) has entered the aggregation unit. The pmf of N_s , $\{P(N_s = n, n = 0, \dots, N - 1)\}$, can be obtained as follows:

$$\begin{aligned} P[N_s = n] &= \sum_{k=0}^{\infty} P[K^{1,a} = kN + n] \\ &= \sum_{k=0}^{\infty} \sum_{i=0}^{\infty} k_i^{1,a} \delta(i - kN - n) \\ &= \sum_{i=0}^{\infty} k_i^{1,a} \sum_{k=-\infty}^{\infty} \delta(i - kN - n) \end{aligned} \tag{35}$$

where $K^{1,a}$ is the number of blocks presented in queue 1 seen at the arrival of a random packet. PASTA property [25] implies that $K^{1,a} = K^1$. $\delta(n)$ is the Kronecker delta function, which equals 1 for $n = 0$ and 0 for all other n , and $\{k_i^1 = 0, \text{ for } i < 0\}$. Now we make use of the following identity:

$$\sum_{k=-\infty}^{\infty} \delta(i - kN - n) = \frac{1}{N} \sum_{s=0}^{N-1} a^{s(i-n)} \tag{36}$$

with: $a = \exp(j\frac{2\pi}{N})$. In words: the right-hand side of (36) equals zero unless the integer $i - n$ is a multiple of N , when it equals unity. Thus,

$$\begin{aligned} P[N_s = n, 0 \leq n \leq N - 1] &= \sum_{i=0}^{\infty} k_i^1 \frac{1}{N} \sum_{s=0}^{N-1} a^{s(i-n)} \\ &= \frac{1}{N} \sum_{s=0}^{N-1} a^{-sn} K^1(a^s) \end{aligned} \tag{37}$$

where $K^1(a^s)$ is $K^1(z)$ evaluated at $z = a^s$.

Obtaining the pmf of N_s by using (37) for each value of n leads to a very long computation time, especially when N becomes large. However, we give an equivalent matrix equation for this relation. This approach reduces the computation time considerably since it gives the pmf of N_s by using only one matrix equation. If P_{N_s} denotes the row vector representing the pmf of N_s , i.e $P_{N_s} = (P(N_s = 0)P(N_s = 1)P(N_s = N - 1))$, and if we define R_{K^1} by: $(K^1(a^0)K^1(a^1) \dots K^1(a^{(N-1)}))$, we will have:

$$P_{N_s} = \frac{R_{K^1}}{N} \times \begin{pmatrix} a^0 & a^0 & a^0 & \dots & a^0 \\ a^0 & a^{-1} & a^{-2} & \dots & a^{-(N-1)} \\ a^0 & a^{-2} & a^{-4} & \dots & a^{-2(N-1)} \\ \dots & & & & \\ a^0 & a^{-(N-1)} & a^{-2(N-1)} & \dots & a^{-(N-1)^2} \end{pmatrix} \tag{38}$$

where the last matrix in 38 is an $N \times N$ matrix. Now, $p_s^{1,1}$ can be obtained easily by: $p_s^{1,1} = P(X > N - N_s)$.

Computation of D_s^2 . Unlike the class 1 case, where a packet cannot be segmented more than once, a class 2 packet may encounter several segmentations before its complete transmission. This is because when a class 2 packet is segmented for the first time, its remaining blocks cannot enter the aggregation unit unless queue 1 is polled again.

If we denote by $p_s^{2,n}$ the probability that a packet is segmented n times, we obtain:

$$D_s^2 = \sum_{n=1}^{\infty} p_s^{2,n} \times (n\tau) \tag{39}$$

However, considering only the first two terms of (39) is sufficient as we will see in the numerical examples. To obtain the pmf of N_s we proceed as in the previous section with the difference that here the number of blocks that enter the aggregation unit before a class 2 packet is equal to the number of blocks presented in queue 1 and queue 2 when the packet arrives (i.e, $K^{1,a} + K^{2,a}$), plus the number of class 1 blocks that arrive during the waiting time of the packet first block (represented by the random variable $N_{b,2}^1$). Now we use the PASTA property $\{K^{c,a} = K^c, c = 1, 2\}$ and we approximate $N_{b,2}^1$ by its mean ($E[N_{b,2}^1] = \lambda_1 E[X] E[D_b^2]$ thanks to Little theorem). Then, by replacing the random variable K^1 with $\{K^1 + K^2 + E[N_{b,2}^1]\}$ in the method presented in the previous section, and by supposing that queue 1 and queue 2 are independent (i.e, K^1 and K^2 are two independent random variables), we can express the pmf of N_s by the following:

$$P [N_s = n, 0 \leq n \leq N - 1] = \frac{1}{N} \sum_{s=0}^{N-1} a^{-sn} \left((a^s)^{E[N_{b,2}^1]} K^1(a^s) K^2(a^s) \right) \tag{40}$$

The last term between parentheses in (40) is the z -transform of $\{K^{1,a} + K^{2,a} + E[N_{b,2}^1]\}$, ($= z^{E[N_{b,2}^1]} K^1(z) K^2(z)$), evaluated at $z = a^s$. Now the first two terms of 39 can be obtained as follows:

$$p_s^{2,1} = P(X > N - N_s) \quad \text{and} \quad p_s^{2,2} = P(X - (N - N_s) > G) \tag{41}$$

where G stands for the gap random variable.

3.4 Extension to $J, \{J > 2\}$, Classes

We explain how to extend the analysis when more than two packet classes are desired.

The filling ratio can be obtained by the same manner used in the case of two classes. However, for the delay analysis of packets belonging to queue i , $\{i = 2, \dots, J\}$, we combine queues $\{1, 2, \dots, i - 1\}$ in a single queue and the analysis is reduced to two queues with respective arrival rates: $\lambda_1 = \sum_{k=1}^{i-1} \lambda_k$, and $\lambda_2 = \lambda_i$.

3.5 The Probabilistic Priority Discipline

In order to overcome the drawbacks of the strict priority discipline that has been used in the analytical model, one may apply a probabilistic algorithm such as the one presented in [16]. For this purpose, a parameter p_i , $1 \leq i \leq J$, $0 \leq p_i \leq 1$, is assigned to each arrival queue i , and a relative weight $r_i = p_i \prod_{j=1}^i (1 - p_{j-1})$, where $p_0 = 0$, is computed. Then, the following steps are applied.

1. At each aggregation cycle, the set of non-empty queues, NQ is determined, and a normalized relative weight, $\tilde{r}_i = \frac{r_i}{\sum_{j \in NQ} r_j}$ is calculated. The latter is regarded as the probability with which queue i is served among all non-empty queues in an aggregation cycle.
2. Fill the aggregate packet from the polled queue in Step 1. If the aggregate packet becomes full, send it to the conversion queue and apply Step 1 to the next aggregation cycle, elsewhere exclude the polled queue from NQ and apply Step 1 to the same aggregation cycle if NQ is not empty, or apply Step 1 to the next aggregation cycle if NQ is empty.

3.6 Numerical Examples

We give some numerical examples showing the usefulness of the model. All the computations (probabilities and means) have been done in double precision. The mean delay and the mean filling ratio are obtained from their corresponding pmfs. We consider the following assumptions.

1. From experimental measurements [23], the size distribution of IP packets has three predominant values: 40 bytes, 552 bytes and 1500 bytes, with the corresponding probabilities 0.6, 0.25 and 0.15 respectively. To discretize the size distribution, we suppose that the size of a random packet is a batch of 40 bytes blocks, and hence the packet size PGF is given by: $\{X(z) = 0.6z + 0.15z^{14} + 0.25z^{38}\}$, where each power of z represents the first integer greater or equal to the division quotient of the corresponding packet size by the block size (e.g., $\lceil \frac{552}{40} \rceil = 14$, $\lceil \cdot \rceil$ is the first integer greater or equal to \cdot).
2. Each node has two classes (real-time applications and non-real-time applications) with proportions 0.6 and 0.4, respectively. The arrival processes of the two classes are Poisson processes with rates λ_1 (packet/s) and λ_2 (packet/s) respectively; the total arrival rate is $\lambda_0 = \lambda_1 + \lambda_2$. In the examples, we suppose that the arrival rates are represented, in Mb/s, by: $\{\theta_c, c = 0, 1, 2\}$, where $c = 0$ represents the case of the combination of queues 1 and 2. It is easy to verify that λ_c is related to θ_c by: $\lambda_c = \frac{\theta_c \times 10^6}{8bE[X]}$. In the rest of the paper, we use θ and θ_0 interchangeably. Note that the choice of two classes in the numerical examples is adopted for comparison purposes only since the model is scalable regardless of the number of classes. Furthermore, Poisson traffic is considered because we aim at proving that the multicast aggregation technique increases the filling ratio of an optical packet. Clearly, this conclusion remains true regardless of the traffic profile.

- The size of the aggregate packet (N blocks) is supposed to be fixed by the operator, and the maximal arrival rate $\theta_{0,max}$ (or simply θ_{max}) is supposed to be known a priori (by effectuating measurements over several time-scales).

Nodes stability condition and stability region. The stability condition of the node is respected if (see 21): $N > E[A_\tau^0]$, with $E[A_\tau^0] = \lambda_0 \tau E[X]$.

stability region. Let the parameter a be the following: $a = E[A_\tau^0]$ (this is the mean of blocks number that arrive during τ). For a given value of N and θ_0 (or simply θ), the parameter a must be strictly less than N to maintain the stability and then we must choose τ according to:

$$\tau_\theta < \frac{N}{\lambda_0 E[X]} \tag{42}$$

where τ_θ is the value of the time-out when operating at θ . 42 defines what we call the stability region at the arrival rate θ . To obtain a desired value of a inside the stability region we choose τ_θ according to: $\tau_\theta = \frac{a}{\lambda_0 E[X]}$. For instance, for $N = 76$ blocks, and $\theta = 900$ Mb/s, (42) implies that the limit of the stability region is $\tau_{max} = 27 \mu s$.

Impact of the time-out. We present in Fig. 5 the impact of τ on the filling ratio. The pmf of the filling ratio is shown for two values of τ ($\tau = 12.5 \mu s$ and $\tau = 25 \mu s$), with $\theta = 900$ Mb/s and $N = 76$. We observe that when τ increases, the probability that the aggregate packets are sent with better filling ratio increases. This is because when τ increases, while remaining inside the stability region, the number of packets presented in queues 1 and 2 at a random epoch increases. Note that for $\tau = 25 \mu s$ the aggregate packets are sent full with probability 0.82952. This is because τ is very close from the stability limit ($27 \mu s$).

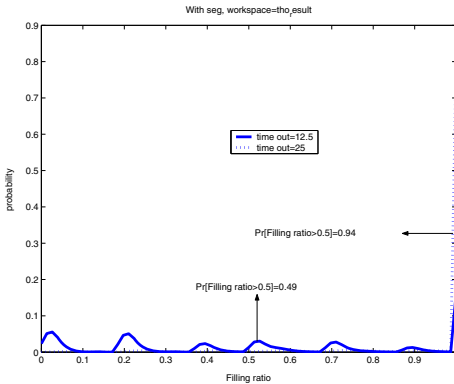


Fig. 5. pmf of the filling ratio

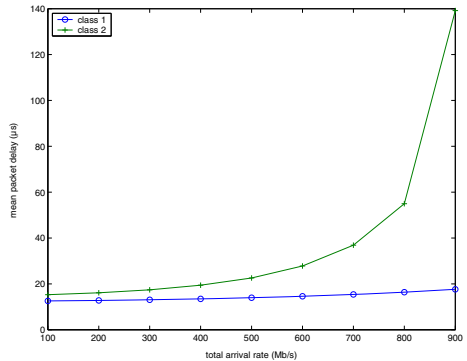


Fig. 6. The mean packet delay as function of the arrival rate θ

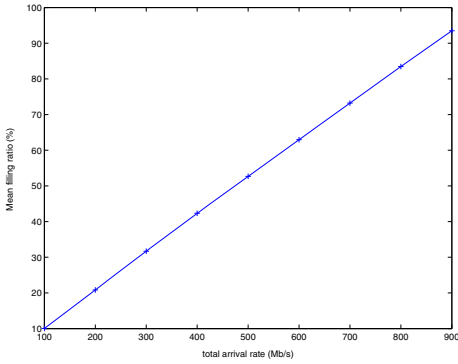


Fig. 7. The mean filling ratio as function of the arrival rate θ

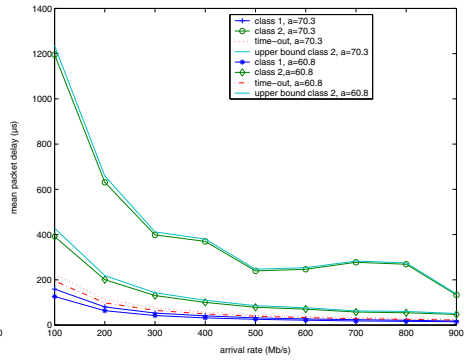


Fig. 8. The mean packet delay in the case of the adaptive τ scenario

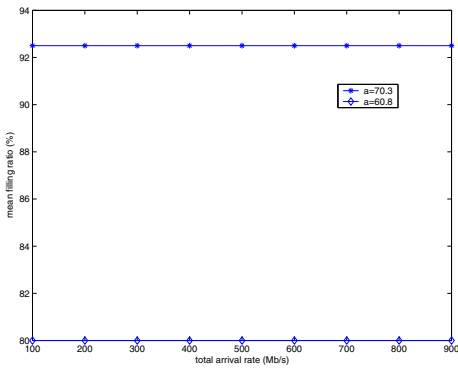


Fig. 9. The mean filling ratio in the case of the adaptive τ scenario

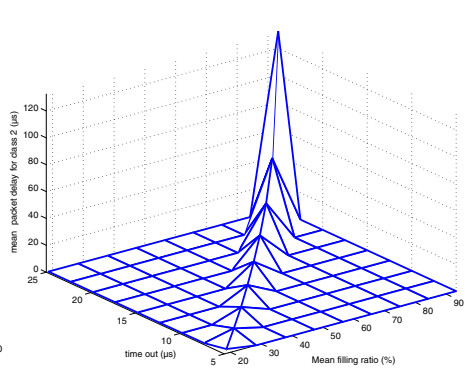


Fig. 10. Class 2 mean packet delays

Effect of the arrival rate. The impact of the arrival rate on both mean packet delay and mean filling ratio is given in Fig. 6 and Fig. 7 respectively. N is fixed to 76 and τ to $25\mu s$. It can be observed that the mean delay of class 1 packets remains approximately unchanged when θ varies, while the mean delay of class 2 packets degrades when θ increases. The mean filling ratio increases also as θ increases. At $\theta = 900$ Mb/s, the mean filling ratio attains 93.506% since at this arrival rate, $\tau = 25 \mu s$ becomes very close to the limit of the stability region. Note that when θ decreases, the enhancement in the delay is compensated by a loss in the filling ratio. This is because τ remains constant. To avoid this limitation, we can adapt the value of τ with respect to the variation of θ in order to conserve a fixed value of the parameter a (obtained from nodes stability), which represents the mean size (in blocks) of the packets that arrive between two consecutive timer expirations. In Fig. 8 we show the effect of a on the mean packet delay (we take $a = 70.3$ blocks and $a = 60.8$ blocks). It is clear that when a decreases

the delay decreases (decreasing a means that for a given θ the time-out τ has a less value which implies less delays). The advantage of the adaptive τ scenario is to maintain the mean filling constant as shown in Fig. 9. We can also deduce that reducing a leads to a decrease in the mean filling ratio as expected (because of the decrease in τ). Finally, Fig. 10 represents how an industrial operator can make use of the aggregation model. If a certain value of the mean filling ratio is desired, then by using the curve we can obtain the value of class 2 mean packet delay (z -axis) and the value of the time-out to setup (y -axis). We can adapt the value of the filling ratio to obtain a desired value of class 2 mean packet delay, while class 1 mean packet delay remains below τ (as shown in Fig. 8).

4 Application to MANS

4.1 Hub Stripping Network: DBORN

The term hub stripping refers to the case where a single node in the ring network, called the hub, drops optical packets. This is the case of DBORN, where the hub can be regarded as the single destination of ring nodes in the transmission phase. DBORN has been initially proposed for asynchronous systems [20,3,4]. However, we consider in this work an hybrid slotted version of the original system. DBORN is an optical metro ring architecture connecting several edge nodes, e.g., metro clients like enterprise, campus or local area networks (LAN), to a regional or core network. The ring consists of a unidirectional fiber split into downstream and upstream channels spectrally disjointed (i.e., on different wavelengths) [3]. The upstream wavelength channels are used for writing (transmitting), while downstream wavelength channels are used for reading (receiving). In a typical scenario, the metro ring has a bit-rate 2.5 Gb/s, 10 Gb/s or 40 Gb/s per wavelength. In order to keep the edge node interface cards as simple as possible, all traffic (external and intra-ring) has to pass the hub. Specifically, no edge node receives or even removes traffic on upstream channels or inserts traffic on downstream channels. Thus, both upstream and downstream channels can be modeled as shared unidirectional buses. Packets circulate around the ring without any electro-optic conversion at intermediate nodes. The hub is responsible of terminating upstream wavelengths and hence, the first node in the upstream bus receives always free slots from the hub. Moreover, the hub electronically processes the packets, which may leave to the backbone or go through the downstream bus to reach their destinations. In the latter case, the ring node must pick up a copy of the signal originating from the hub by means of a splitter in order to recover its corresponding packets by processing them electronically. In the following, we consider that each node is equipped with one fixed transmitter and as many fixed receivers as reception channels, i.e., for each node we assign only one transmission wavelength at the upstream bus.

Two MAC protocols may be used. The empty slot procedure and a slot reservation mechanism.

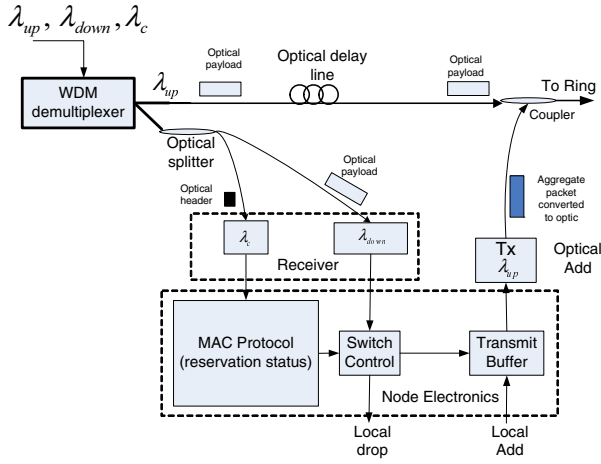


Fig. 11. The ring node architecture of slotted DBORN

In the case of empty slot procedure, the slot header is detected to determine the status of the slot (i.e., empty/full) and a node may transmit on every empty slot.

In the case of the reservation approach, we implement a slot reservation mechanism at the upstream bus. Indeed, a fixed number of slots are reserved for each node. We suppose that the slot assignment is performed in the hub which writes the address of the node, for which the slot is reserved, in the slot's header. Hence, when a node receives an incoming slot, it detects the header to determine the status of the slot (empty/full) and the reservation information to decide whether to transmit or not. In addition to its reserved slots, the node can use empty slots reserved to any of its upstreams. This is because all slots are emptied by the hub before being sent on the upstream bus. This interesting feature of DBORN makes it possible to avoid the inefficiency behavior of a TDMA scheme. For instance, if a node i does not fill a reserved slot because its local queue is empty, then any downstream node which transmits on channel λ_{e_i} can use this slot for transmission because the hub will empty the slot before it reaches node i again. This enables efficient use of the available bandwidth in the case of non uniform traffic. Furthermore, at overloaded conditions, i.e., when the local queues of all nodes are always non empty, the MAC protocol reduces to a TDMA scheme, since each node will consume all its reserved slots for transmission.

Note that in order to process the control information, only the control channel is converted to the electrical domain at each ring node, while the bulk of user information remains in the optical domain until it reaches the hub which is viewed as the destination of upstream data. This is in conformity with the notion of all-optical (or transparent) networks in literature (e.g., [14]). The corresponding network node architecture is given in Fig. 11, where λ_{up} , λ_{down} and λ_c represent the upstream bus, the downstream bus and the control channel respectively. The slots in the control channel have a locked timing relationship to the data slots

and arrive earlier at each node by a fixed amount of time (this is achieved via an optical delay line, see Fig. 11) allowing the process of the control slot content.

At the downstream reading bus, ring nodes preserve the same behavior initially proposed in DBORN and hence, the optical signal is split and IP packets are recovered at each node. The latter drops packets which are not destined to it. This means that DBORN supports multicast without addition of any complexity in its MAC protocol and hence, it represents an interesting application of the multicast packet aggregation method presented in this work.

5 Application to WANs

The multicast aggregation technique analyzed throughout this paper can be easily adapted to the studied MANs. On one hand, the support of multicast traffic is facilitated due to the simplicity of ring architecture. On the other hand, aggregation of IP packets belonging to different QoS classes in one aggregate packet is justified since there is no packet loss inside such ring networks. This is because in-transit traffic has always higher priority than local traffic at intermediate nodes.

The problem of multicast handling and QoS support in WAN may introduce some adjustments to the proposed aggregation techniques because wide area networks have a mesh topology in general. The scenario proposed in [18]

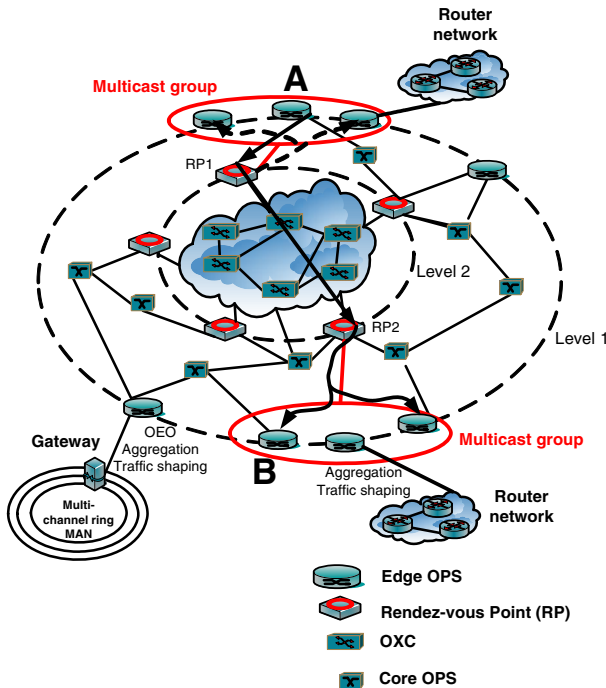


Fig. 12. Possible WAN architecture

is adopted. Indeed, optical packet switching provided through optical packet switches (OPSs) and circuit switching ensured by OXCs (Optical Cross-Connects), coexist within the network. The former is deployed in areas where granularity is below the wavelength level, while the latter interconnects high-capacity points that will fully utilize the channel capacity in the core of the network. To do this, some optical channels (wavelength paths) may interconnect OXCs. Other channels might be reserved to OPSs to support optical packet transmission. Once the technology matures and the need for a more flexible fully IP-centric network is dominant, optical packet switches may replace the OXCs, or alternatively reduce their size and cost significantly, as the wavelength channels are more efficiently used and hence, equipment requirements are reduced. Furthermore, we propose a network with two hierarchy levels. The first level is constituted from edge and core OPSs. Edge OPSs differ from core OPSs in that they are connected to client layer networks, such as IP networks and to metropolitan area networks such as the networks studied in this work. Edge OPSs are responsible of performing IP packet aggregation in order to improve bandwidth efficiency. Indeed, optical packets received through MANs must be converted to electronic in order to join a new aggregation process. The latter must take into consideration the two fundamental questions (multicast and QoS) in the context of the WAN architecture. This is may be given as follows. In WANs the number of edge nodes is much greater than that in MANs and hence, aggregating IP packets regardless of their destinations leads to generating a big number of broadcast optical packets which may waste the network resources. Instead, we suppose that edge nodes are separated in multicast groups. Each multicast group has a designed router, called Rendez-vous point (RP).

The OPS is responsible of communicating with the level-1 hierarchy nodes, while the interconnection between RPs through lightpaths between OXCs makes the level-2 hierarchy. An IP-centric control plane is responsible of four major tasks. 1) Constructing the multicast groups by using the IGMP protocol [5]. 2) Electing an RP for each group by using an approach similar to that of the PIM-SM multicast protocol [13]. 3) Constructing lightpaths between RPs. 4) Constructing a shared multicast tree between nodes of each group and fixed lightpaths between RPs. GMPLS [1] is a candidate to perform these tasks after doing the necessary extensions. Now each edge node performs a separate aggregation process per RP. That is, IP packets destined to edge nodes belonging to the same multicast group are aggregated together. If the multicast optical packet is destined to the designated RP of the multicast group, the RP multicasts it on the shared multicast tree, elsewhere the RP sends the packet to the corresponding RP through a lightpath on the level-2 hierarchy and the latter multicasts it on the shared tree. For instance, in Fig. 12, suppose that node *A* wishes to send two optical packets: one for its group and another one for node *B* and other nodes in a different multicast group. In the former case, the packet is forwarded to RP_1 which multicasts it through its multicast tree (dashed arrows). In the latter case, RP_1 sends the packet to RP_2 which multicasts it on its shared tree to get the destination nodes including node *B*.

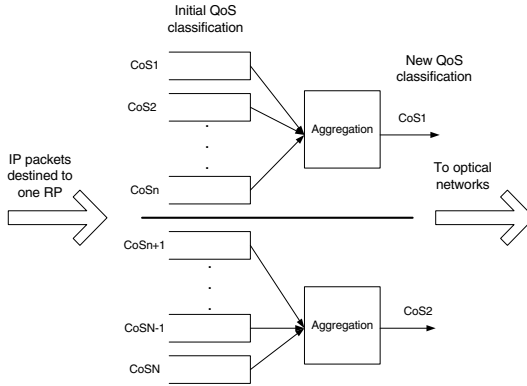


Fig. 13. A possible QoS classification

The QoS support must consider that OPSs have limited optical buffering capacity, in terms of fiber delay lines¹ and hence it may be important to generate aggregate packets with several classes of service, contrary to the aggregation in MANs, in order to reduce packet loss of higher priority traffic. Typically, four QoS classes may be sufficient. However, as the number of classes increases as the complexity of the RPs increases where separate control information, such as restoration of lightpaths in case of failure, must be guaranteed for each class. In order to reduce this complexity, two QoS classes may be adopted as shown in Fig. 13.

6 Conclusion

We propose and analyze a novel approach for efficiently supporting IP packets in a slotted WDM optical layer with several QoS requirements. A simple analytical model, allowing the evaluation of IP packets aggregation delay and the bandwidth efficiency, has been presented. The results showed an increase in the bandwidth efficiency when using the aggregation compared to the standard approach. Concerning IP packets aggregation delay, a trade-off with the bandwidth efficiency results by modifying the value of the parameter a . The QoS support mechanism based on assigning higher aggregation priorities for higher QoS classes, has been evaluated by means of an analytical study. The application of the aggregation technique has been shown in the context of MANs and WANs, respectively.

References

1. Banerjee, A.: Generalized multiprotocol label switching: An overview of signaling enhancements and recovery techniques. *IEEE Comm. Mag.* 39(7), 144–151 (2001)
2. Bengi, K.: Access protocols for an efficient and fair packet-switched IP-over-WDM metro network. *Computer Networks* 44(2), 247–265 (2004)

¹ Fiber delay lines are used due to the absence of random access memory in optic.

3. Bouabdallah, N., et al.: Resolving the fairness issue in bus-based optical access networks. *IEEE Commun. Mag.* 42(11) (November 12-18, 2004)
4. Bouabdallah, N., Beylot, A.-L., Dotaro, E., Pujolle, G.: Resolving the Fairness Issues in Bus-Based Optical Access Networks. *IEEE J. Select. Areas Commun.* 23(8) (August 2005)
5. Cain, B., et al.: Internet Group Management Protocol, Version 3, RFC 3376, <http://www.ietf.org/rfc/rfc3376.txt?number=3376>
6. Careglio, D., Pareta, J.S., Spadaro, S.: Optical slot size dimensioning in IP/MPLS over OPS networks. In: 7th International Conference on Telecommunications. *CONTEL 2003*, Zagreb, Croatia, pp. 759–764 (2003)
7. Castel, H., Chaitou, M.: Performance Analysis of an Optical Man ring. In: 7th Informatics Telecommunication Conference, Boca Raton Florida (2004)
8. Chaitou, M., Hébuterne, G., Castel, H.: On Aggregation in Almost All Optical Networks. In: Second IFIP International Conference on Wireless and Optical Communications Networks, *WOCN 2005*, Dubai, United Arab Emirates UAE, pp. 210–216 (2005)
9. Chaitou, M.: Performance of multicast packet aggregation with quality of service support in all-optical packet-switched ring networks. PHD thesis, Evry, France (2006)
10. DeCusatis, C.: Optical Wavelength Division Multiplexing for data communication networks. *Fiber Optic Data Communication*, 134–215 (2002)
11. Detti, A., Eramo, V., Listanti, M.: Performance Evaluation of a New Technique for IP Support in a WDM Optical Network: Optical Composite Burst Switching (OCBS). *IEEE J. Lightwave Technol.* 20(2), 154–165 (2002)
12. Dittmann, L., et al.: The European IST project DAVID: a viable approach towards optical packet switching. *IEEE J. Select. Areas Commun.* 21(7) (September 2003)
13. Estrin, D., et al.: Protocol Independent Multicast-Sparse Mode (PIM-SM): Protocol Specification. RFC 2362, <http://www.ietf.org/rfc/rfc2362.txt?number=2362>
14. Gambini, P., et al.: Transparent optical packet switching: network architecture and demonstrators in the KEOPS project. *IEEE J. Select. Areas Commun.* 17(7) (September 1998)
15. Hébuterne, G., Castel, H.: Packet aggregation in all-optical networks. In: *Proc. First Int. Conf. Optical Commun. and Networks*, Singapore, pp. 114–121 (2002)
16. Jiang, Y., Tham, C., Ko, C.: A probabilistic priority scheduling discipline for high speed networks. In: *IEEE Workshop on High Performance Switching and Routing*, May 2001, pp. 1–5 (2001)
17. Jiang, Y., Tham, C., Ko, C.: A probabilistic priority scheduling discipline for multi-service networks. *Computer Communications* 25(13) (August 2002)
18. O'Mahony, M.J., Politi, C., Klonidis, D., Nejabati, R., Simeonidou, D.: Future optical networks. *IEEE J. Lightwave Technol.* 24, 4684–4696 (2006)
19. Mortensen, B.B.: Packetisation in Optical packet switch fabrics using adaptive timeout values. In: *Workshop on High Performance Switching and Routing*, Poznan, Poland (June 2006)
20. Sauze, N.L., et al.: A novel, low cost optical packet metropolitan ring architecture. In: *European Conference on Optical Communication (ECOC 2001)*, Amsterdam, October 2001, vol. 3, pp. 66–67 (2001)
21. Scheutzwow, M., Seeling, P., Maier, M., Reisslein, M.: Multicast capacity of packet-switched ring WDM networks. In: *Proc. IEEE INFOCOM*, vol. 1, pp. 706–717 (2005)

22. Srivatsa, A., et al.: CSMA/CA MAC protocols for IP-HORNET: an IP over WDM metropolitan area ring network. In: Proceedings of GLOBECOM 2000, San Francisco, CA (2000)
23. Thompson, K., Miller, G.J., Wilder, R.: Wide-area Internet Traffic Patterns and Characteristics. *IEEE Network* 11(6), 10–23 (1997)
24. Uscumlic, B., Gravey, A., Morvan, M., Gravey, P.: Impact of Peer-to-Peer traffic on the Efficiency of optical packet rings. In: *IEEE Broadnets 2008*, UK, London, September 8-11, pp. 146–155 (2008)
25. Wolff, R.W.: *Stochastic modeling and the theory of queues*. Prentice-Hall, London (1989)
26. Yao, S., Mukherjee, B., Dixit, S.: Advances in photonic packet switching:an overview. *IEEE Commun. Mag.* 38(2), 84–94 (2000)